



A MODEL OF STIFFNESS NON-LINEARITY IN FIBROUS MATERIAL DYNAMICS

H. J. RICE AND A. A. TORRANCE

Department of Mechanical and Manufacturing Engineering, Trinity College Dublin, Ireland

AND

G. EIKELMAN

Department of Mechanical Engineering, Technical University of Darmstadt, Germany

(Received 31 July 1997, and in final form 17 November 1997)

1. INTRODUCTION

In the study of aircraft interior vibroacoustics the major dissipative mechanism at propeller tone frequencies can be attributed to the dynamic interaction of the thermal insulating layer in the cabin walls with the ambient vibration and acoustic fields. The most popular materials currently used in these designs are those in the form of glass fibre blankets. At these low frequencies the dynamical behaviour of the material is bi-phasal incorporating both a fluid and an interacting structural or frame element. Although considerable work has been reported on the modelling of these materials (see, for example, the publications of Göransson [1], and Rice and Göransson [2] based primarily on fundamental work by Biot [3] and Zwicker and Kosten [4]) the effect of frame non-linearity has been ignored. Pritz [5], however, has pointed out that even at strain levels as low as 10^{-4} , these effects can be significant and typical fibrous materials can be expected to exhibit a softening stiffness characteristic. He then reported on some vacuum based dynamical tests conducted on denser architectural grade material and proposes functional models based on random tests which relate transmissibility resonance frequencies and amplitudes to dynamic mean square strain levels. In a previous paper by Rice *et al.* [6] similar tests were performed on a fibrous test sample used in the aerospace industry under atmospheric test conditions and the characteristic softening non-linearity was again noted. In that paper an attempt was made to fit a (symmetric) functional model to the instantaneous response levels with partial success.

In this letter a model of the stiffness non-linearity based on purely physical considerations is proposed and is shown to agree well with dynamical measurements performed on a fibrous material sample used in an aerospace application.

2. ANALYSIS

In this analysis only the stiffness element of the non-linearity will be considered while the damping will be modelled in the usual way as a linear viscous process.

Observation of the fibrous wool in a low power binocular microscope shows that it is composed of layers, up to 1 mm thick, of glass fibres orientated mostly in one distinct plane (xy plane). The layers are linked by tangles of fibres aligned roughly perpendicular to this plane (z direction). When sufficient stress is applied in the z direction to give strains of around 5%, the layers can be seen to deform as a series of platelets of varying size and thickness, loaded in the centre and restrained at the edges as shown in Figure 1. But, at lower strains, additional restraint to the bending of these platelets is provided by single fibres in the z direction which hook onto adjacent platelets like “Velcro”. The response

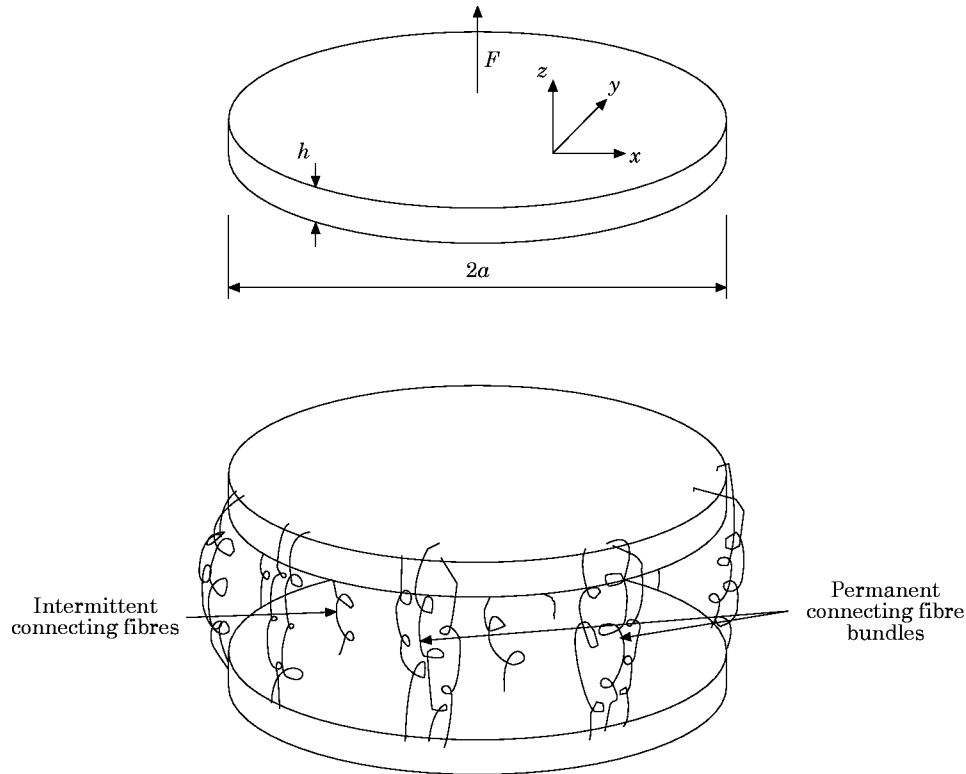


Figure 1. Platelet model of fibrous structure.

of the wool to out-of-plane loading at high tensile strains can therefore be investigated by idealizing it as an array of deforming discs loaded centrally and restrained at the edges by attachments to neighbouring discs. This interpretation is similar to some of the methods used for modelling the elastic properties of foams [7]. At low strains, additional stiffness is provided by the individual links within the plates, which disconnect progressively as strain increases. Both of these stiffness mechanisms may be accounted for as follows.

1.1. Flexion of platelets

For a circular of modulus E loaded as shown by the force F , and simply supported at the edges, the deflection δ of the centre is given by

$$\delta = 3F(1 - \nu^2)(3 + \nu)a^2/2\pi Eh^3(1 + \nu) \quad (1)$$

Since, for glass wool, $\nu = 0$, this reduces to

$$\sigma = 9Fa^2/2\pi Eh^3 = (9/2\pi)(\sigma h/E)(a/h)^4, \quad (2)$$

where $\sigma = F/a^2$, which gives, on dividing through by h and setting $\varepsilon = \delta/h$,

$$\sigma = (2\pi/9)(h/a)^4 E\varepsilon. \quad (3)$$

Let one now suppose that a fraction f_i of the wool fibres are oriented in the z direction, whilst the remainder are oriented in the xy plane. If the density of the wool relative to

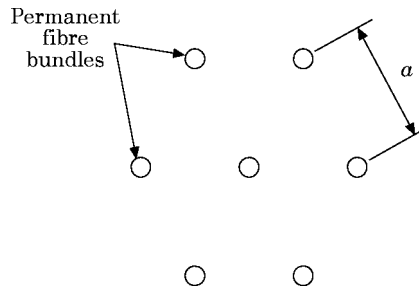


Figure 2. Arrangement of permanent cross-links.

the glass at zero strain is ρ_0 , then the in-plane modulus, by analogy with a foam [7] is given by

$$E = E_g \rho_0^2 (1 - f_i)^2. \tag{4}$$

Since the density ρ_0 will change with strain, a more general value for the modulus will be

$$E = E_g \rho_0^2 (1 - f_i)^2 / (1 + \varepsilon)^2 \tag{5}$$

The number of fibres in the z direction per unit area, n , is

$$n = \rho_0 f_i / \pi r^2, \tag{6}$$

where r is the radius of the fibre. If one supposes that half these fibres are grouped in bundles to form links between the flexing platelets of Figure 1, one can develop a relationship for (h/a) . The cross-links between layers of wool can be idealized as a regular hexagonal array of fibres (cf. Figure 2). If there are p fibres per cross-link, there are $4p$ cross links per hexagonal cell, and thus

$$a = \sqrt{4p/n\sqrt{3}} = 2r\sqrt{2\pi p/\rho_0 f_i \sqrt{3}}. \tag{7}$$

If one now assumes that the layers of wool consist of bundles of p fibres stacked as in Figure 3, one finds that

$$h = r\sqrt{\pi p/\rho_0(1 - f_i)}, \tag{8}$$

which yields

$$h/a = \sqrt{f_i \sqrt{3}/4(1 - f_i)}. \tag{9}$$

Combining equations (3), (6) and (9) gives a value for the modulus due to flexion of the platelets.

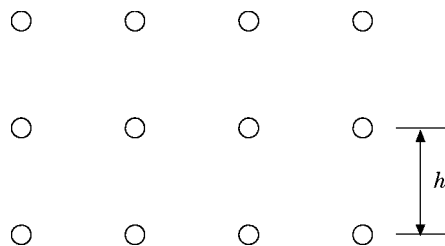


Figure 3. Fibre bundle stacking.

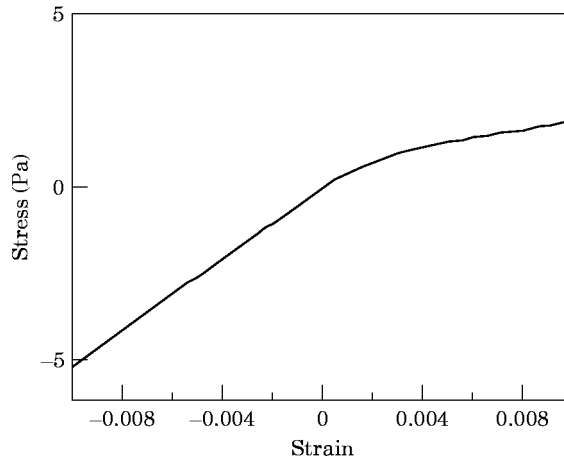


Figure 4. Stress-strain curve for the fibrous material.

1.2. Deformation of fibres

Provided none of the fibres linking the platelets become unhooked from one of the platelets, their stiffness could be modelled in the same way as that of a foam:

$$\sigma = (E_g \rho_0^2 f_f^2 / 4(1 + \varepsilon)^2) \varepsilon \quad (10)$$

However, whilst this may apply in compression, in tension the fibres will progressively unhook themselves as strain increases. This may be represented mathematically by a Weibull [8] distribution of strengths as the probability P_s that a link will survive a strain ε :

$$P_s = e^{-(\varepsilon/\varepsilon_0)^\beta} \quad (11)$$

where ε_0 is the characteristic strain at which 62% of the fibres have failed, and β is the modulus of the strength distribution. The overall equation for response to stress is then

$$\sigma = \frac{E_g \rho_0^2 f_f^2}{(1 + \varepsilon)^2} \left(\frac{\pi}{24} + \frac{P_s}{4} \right) \varepsilon, \quad (12)$$

where P_s is given by equation (10) in tension, but is equal to 1 in compression. With $f_f = 0.03$, $\rho_0 = 0.0044$, $E_g = 76$ GPa, $\varepsilon_0 = 0.004$ and $\beta = 1$, one obtains the stress-strain curve shown in Figure 4.

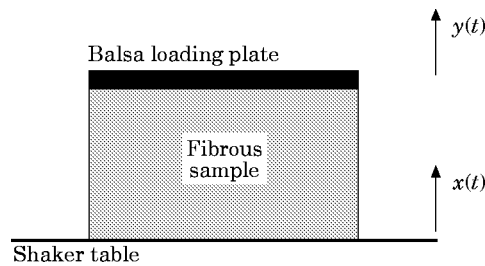


Figure 5. Seismic mass test set-up.

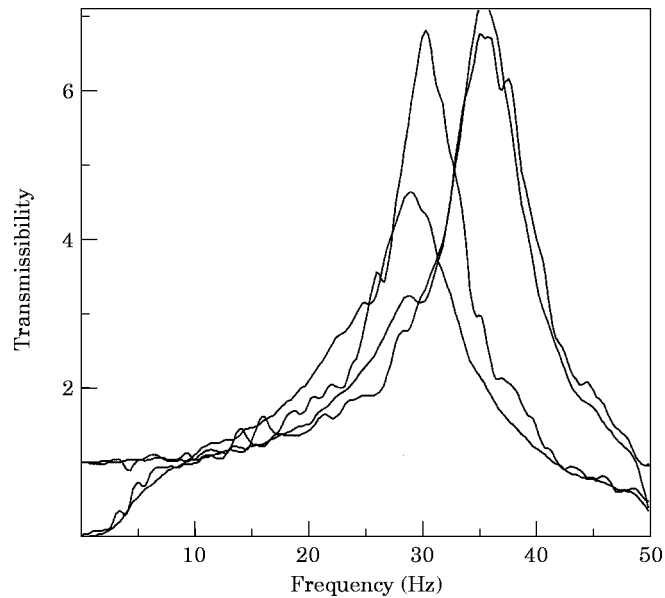


Figure 6. Frequency responses under high and low excitation levels. The smoother curves are the simulated ones.

3. EXPERIMENT

3.1. Set-up

In order to validate the above theory, a simple seismic test shown schematically in Figure 5 was conducted under “soft” vacuum conditions (<20 Pa). This was necessary to remove the significant stiffness and damping effects generated by entrained air which for the present set-up rendered the primary resonance almost to be unobservable.

The dynamics of the fibrous material was assessed by measuring the effective linear frequency response of the plate with respect to the shaker table motion under a range of excitation levels. The excitation was band-limited and random and was generated by an HP 35665A spectrum analyzer which was also used to sample, ensemble average and calculate the transmissibility.

As the test material was highly compliant a light balsa loading plate of mass 0.97 g was used in order to achieve a resonance frequency as close as possible to realistic blade-passing frequencies. A non-contacting laser vibrometer was used to measure the response while a standard accelerometer was used to measure the motion of the base plate. The sample dimensions were 55 mm × 55 mm × 19 mm (height). By using this arrangement it was possible to achieve a clear resonance peak which exhibited amplitude sensitivity at frequencies in the region of 40 Hz although there is some evidence of a spurious peak probably induced by sample mounting or stability problems.

3.2. Numerical simulation and results

In order to investigate the validity of the dynamic stress–strain model proposed in section 2, fourth order Runge–Kutta simulations of the governing system differential equation

$$(m + M/3)\ddot{u}_r + c\dot{u}_r + f(\varepsilon) = -(m + M/2)\ddot{u}_b \quad (13)$$

were performed where u_r represents the relative motion $u_p - u_b$ of the loading plate with respect to the excitation table, m is the mass of the loading plate and M is the total mass of the test sample. It should be understood that the viscous damping term here, $c\dot{u}_r$, is a gross approximation to the dissipation within the fibres and in fact should be expected to vary with response level [5, 6]. However, in order to focus on the stiffness issue it has been assumed to be constant for the present study. The validity of equation (13) depends on the assumption that the strain is constant with respect to the z direction and varies only with time. The restoring stiffness force $f(\varepsilon)$ is calculated directly from the instantaneous stress calculated by using relationship (12) with

$$f = A\sigma, \quad (14)$$

which depends on a strain value given by

$$\varepsilon = U_r/L. \quad (15)$$

Simulations were then performed with excitation records \ddot{u}_b used as input which were identical to those which were also used in a series of experiments. Thus, modelled transmissibilities calculated by using

$$T(\omega) = 1 - \omega^2 U_r(\omega) / \dot{U}_b(\omega) \quad (16)$$

could then be compared with experimentally observed transmissibilities to test the validity of the stiffness model. This comparison is shown in Figure 6 for nominally high and low levels of excitation (generating r.m.s. strains of the order of 0.008 and 0.002 respectively) and for the parameter values set out above.

4. RESULTS AND DISCUSSION

As can be seen the proposed model certainly has the capacity to model the softening phenomenon correctly when using parameter values which are compatible with direct measurement (E_g, ρ_0) or observation ($f_t, \varepsilon_0, \beta$). $\beta = 1$ represents an appropriate Weibull modulus for this type of heterogeneous material and implies that the breaking strains of the fibres follow a Poisson distribution which is scaled by the factor ε_0 . With regard to the material stress-strain relationship itself the asymmetric nature has the capability of generating both an appropriate system response and a satisfying physical model. Such asymmetry can prove difficult to identify experimentally in dynamic tests which may explain much of the shortcomings of the results presented in reference [6] where a symmetric exponentially based stiffness characteristic was inferred for this type of structure. Clearly the exponential nature of the stiffness relationship modelled here by the Weibull process appears to be an essential element in understanding the dynamic behaviour of the material and it is interesting to note that some more naive models (softening Duffing) used in test simulations for this failed due to static instability when the excitation level was varied over the testing ranges. Finally although a linear damping model was used here, it is clear that some non-linearity in the damping process should also be considered as reported in references [5, 6] to further improve the model performance. This will form the basis of further work.

ACKNOWLEDGMENT

The authors wish to acknowledge the useful commentary of P. Göransson of the Marcus Wallenberg Laboratory, Department of Vehicle Engineering, KTH, Stockholm.

REFERENCES

1. P. GÖRANSSON 1997 *International Journal for Numerical Methods in Engineering*. A 3D, symmetric, finite element formulation of the Biot equations for a fluid saturated, linear, elastic porous medium.
2. H. J. RICE and P. GÖRANSSON 1997 in *Modern Practice in Stress and Vibration Analysis, Dublin, 3–5 September, Institute of Physics*, 185–191. Modelling of damping in porous media at low frequencies.
3. M. A. BIOT 1956 *Journal of the Acoustical Society of America* **28**, 168–178. Theory of propagation of elastic waves in a fluid-saturated porous solid. I. Low frequency range.
4. C. ZWIKKER and C. W. KOSTEN 1949 *Sound Absorbing Materials*. New York: Elsevier.
5. T. PRITZ 1990 *Journal of Sound and Vibration* **136**, 263–274. Non-linear of frame dynamic characteristics of mineral and glass wool materials.
6. H. J. RICE, J. A. FITZPATRICK and K. W. GROGAN 1994 in *Materials for noise and vibration control* (editors P. K. Raju and R. F. Gibson) New York, American Society of Mechanical Engineers, 27–34. Identification of non-linear characteristics of a thermal insulation material.
7. N. C. HILYARD 1982 *Mechanics of Cellular Plastics*. London: Applied Science Publishers.
8. W. E. C. CREYKE, I. E. J. SAINSBURY and R. MORRELLI 1982 *Design with Non-Ductile materials*. Applied Science Publishers.